Environmental Science & Technology

pubs.acs.org/est

Article

Design of Ionic Liquids for Fluorinated Gas Absorption: COSMO-RS Selection and Solubility Experiments

Julio E. Sosa, Rubén Santiago, Andres E. Redondo, Jocasta Avila, Luiz F. Lepre, Margarida Costa Gomes, João M. M. Araújo, José Palomar,* and Ana B. Pereiro*

Cite This: *Environ. Sci. Technol.* 2022, 56, 5898−5909

Read Online

ACCESS | Metrics & More | Article Recommendations | Supporting Information

ABSTRACT: In recent years, the fight against climate change and the mitigation of the impact of fluorinated gases (F-gases) on the atmosphere is a global concern. Development of technologies that help to efficiently separate and recycle hydrofluorocarbons (HFCs) at the end of the refrigeration and air conditioning equipment life is a priority. The technological development is important to stimulate the F-gas capture, specifically difluoromethane (R-32) and 1,1,1,2-tetrafluoroethane (R-134a), due to their high global warming potential. In this work, the COSMO-RS method is used to analyze the solute−solvent interactions and to determine Henry's constants of R-32 and R-134a in more than 600 ionic liquids. The three most performant ionic liquids were selected on the basis of COSMO-RS calculations, and F-gas absorption equilibrium isotherms were measured using gravimetric and volumetric methods. Experimental results are in good agreement with COSMO-RS predictions, with the ionic liquid tributyl(ethyl)phosphonium diethyl phosphate, $[P_{2444}][C_2C_2PO_4]$, being the salt presenting the highest absorption capacities in molar and mass units compared to salts previously tested. The other two ionic liquids selected, trihexyltetradecylphosphonium glycinate, $[P_{66614}][C_2NO_2]$, and trihexyl(tetradecyl)phosphonium 2-cyano-pyrrole, $[P_{66614}][CNPyr]$, may be competitive as far as their absorption capacities are concerned. Future works will be guided on evaluating the performance of these ionic liquids at an industrial scale by means of process simulations, in order to elucidate the role in process efficiency of other relevant absorbent properties such as viscosity, molar weight, or specific heat.

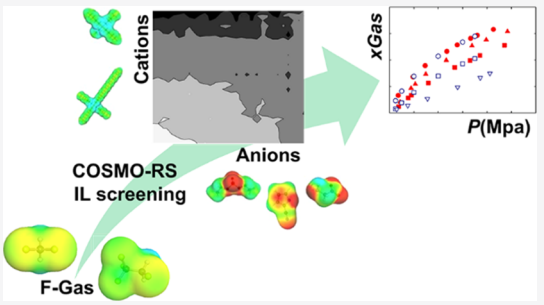

KEYWORDS: *fluorinated gases, greenhouse gases, ionic liquids, COSMO-RS, absorption processes*

1. INTRODUCTION

The exponential growth of fluorinated greenhouse gases is a concern of the European Union since 2014.[1,2] Then, European Commission proposes a progressive reduction and substitution of these greenhouse gases through the EU regulation (no. 517/2014) and the Kigali amendment to the Montreal Protocol signed in 2016. F-gases account for 3.0% of greenhouse gas emissions in 2019.[1,2] However, these gases have a global warming power up to 23 000 times higher than CO_2 and an atmospheric lifetime up to 50 000 years.[1] These gases are widely used in aerosols, refrigeration systems, defoamers, and in the air conditioning equipment of more than 80% of the world's commercial vehicles.[2,3] In addition, in the European Union, about 19 million refrigeration equipment each year have completed their life cycle,[4] generating uncontrollable F-gas emissions of approximately 26 million tons of CO_2 equivalent.[4,5] These emissions are mainly due to the state of the equipment, operating leaks, and the mismanagement that is being given to this equipment after completing its life cycle.[6,7] The effect on climate change of these gases is proportional to the amount emitted. As a consequence of emissions, the degradation of F-gases (e.g., the decomposition of the fluorocarbons HFC-134a, HCFC-123, and HCFC-124) in the atmosphere generates harmful byproducts, such as trifluoroacetic acid (TFA) or HF.[3,8] These compounds are persistent to natural degradation processes and are released into the environment by precipitation.[8−10] TFA acidifies water, is highly toxic upon accumulation in the ecosystems, can irritate tissues, skin, and could have an impact on human health.[11−13] Therefore, efforts to mitigate the impacts of F-gases must be prioritized, seeking alternatives based on sustainable processes for the capture, recovery, and recycling of F-gases. Taking into account the most used F-gases in commercial refrigerants at European level,[14,15] we have chosen in this study the most used F-gases in domestic refrigeration: R-32 (difluoromethane) and R-134a (1,1,1,2-tetrafluoroethane).

Partial recovery for F-gas has been proposed through their capture using porous solid matrices such as activated carbons

Received: January 12, 2022
Revised: March 14, 2022
Accepted: March 17, 2022
Published: April 18, 2022

https://doi.org/10.1021/acs.est.2c00051
Environ. Sci. Technol. 2022, 56, 5898−5909

and metal organic frameworks, taking advantage of the variety of functional groups, pore size, and surface area of these materials.[16,17] Many of these studies have limited application as the cost of production of the porous solid matrices is too high to allow their use at the industrial scale. Therefore, there is a great interest in looking for alternatives to recover the F-gases in the sense of a circular economy, at the end of the life cycles of the equipment containing them.

Ionic liquids (ILs) are salts in the liquid state, recognized in many cases as environmentally friendly solvents. These compounds present exceptional properties, such as negligible vapor pressure, low melting point, and high thermal and electrochemical stability.[18,19] Moreover, they are considered designer solvents because the careful selection of different cations and anions allows us to obtain the desired properties for a specific industrial application. ILs have been considered as alternatives to conventional solvents for various separation processes[19,20] including mixtures of the F-gases studied in this work (R-32 and R-134a).[21−30] Most of the ILs used are based on *bis*-(trifluoromethylsulfonyl)imide[22−24,27] and sulfonate[26,27,30,31] anions, but salts containing fluorinated moieties in the anion or in the cations have also been successfully studied.[28−30] The high HFC solubility in fluorinated ILs (FILs) has been related to hydrogen bonding between solute and solvent molecules in the liquid mixture[29,30,32] but also to favorable entropic effects due to the larger free volume.[29,32] In addition, it has been found that the solubility of F-gases in ILs depends on the structure and size of each F-gas, making the IL selection specific for each F-gas mixture. Thus, it has been demonstrated that the selectivity for the mixture R-134a + R-32 was improved by utilizing FILs,[30] demonstrating that both the cation and anion are determinant to design a suitable solvent for fluorinated greenhouse gas capture by favoring solute−solvent interactions and/or entropic changes for separation.

In the last years, a successful multiscale research strategy was validated for the development of new gas separation processes based on ILs, integrating molecular modeling, experimental essays, and process simulation.[33,34] The first stage allows the selection of the most promising ILs by means COSMO-RS calculations.[34−36] A wide IL database (more than 600 cation/anion combinations) is used to perform a preliminary screening of favorable thermodynamic and kinetic properties for the solute−solvent mixtures,[37] instead of time-consuming and costly experimental tests. Specifically, Henry's law constant (K_H) has been widely used as the main thermodynamic parameter for the IL absorbent selection,[38,39] due to its main role in solvent consumption, energy duty, and operating and investment costs of industrial operation.[40,41] Additionally, the COSMO-RS method is used to gain a deeper understanding of gas absorption phenomena in ILs from a molecular point of view. Thus, it has been found that gas solubility in ILs is commonly governed by absorption enthalpy.[34,42,43] The COSMO-RS method provides the intermolecular interaction (electrostatic, hydrogen bond, and van der Waals) contribution to the excess enthalpy of the solute + solvent mixture, allowing for the rational design of the IL structure to promote the chemical affinity between the components in absorption media.[44−46] In the second stage, selected ILs are experimentally evaluated in the absorption process by measuring gas−liquid equilibria data at different temperature and pressure operating conditions.[35,47,48] Thus, key parameters for the design of the industrial absorption process obtained such as absorption isotherms and diffusivities.[49,50] In the last stage, the performance of selected ILs at the process scale is evaluated by modeling the absorption and desorption operations using COSMO-based/Aspen methodology,[33] in order to perform a techno-economic analysis and to compare with the available technology. It was widely used in different gas capture applications based on ILs such as acetylene,[39] CO_2,[51] and H_2S,[41] among others. In fact, the COSMO-based/Aspen methodology was recently applied to evaluate the absorption process of fluorinated gases using those ILs previously experimentally tested in the literature,[20] obtaining that FILs/ILs based on sulfonate and carboxylate anions present the best process performance for F-gas capture.

In this work, the multiscale research strategy is used to design new ILs with enhanced thermodynamic properties for the absorption of two relevant fluorinated gases (R-134a and R-32), respect to those previously tested in the literature. For this purpose, the COSMO-RS method is applied to perform a massive K_H screening among a wide database of cations (24) and anions (28), including those ILs previously tested in literature, for comparison purposes. In order to gain a deeper insight of the absorption phenomena of R-134a and R-32 compounds in ILs, the excess enthalpy, entropy, and Gibbs energy of solute−solvent mixtures are calculated, completing COSMO-RS analysis by obtaining the intermolecular interaction contributions to the mixing behavior.

From the current computational analysis, we will select ILs showing promising F-gas absorption capacities and we will experimentally evaluate them using gravimetric and isochoric saturation methods at different temperatures and partial pressures of gas. The results will be compared with Henry's law constants previously reported in the literature for other ILs to confirm the successful selection of alternative ILs for F-gas capture.

2. MATERIALS AND METHODS

2.1. COSMO-RS Calculations. First, the geometries of all the ILs included in this work were calculated to their minimum energy structure (optimized) using Turbomole v.7.4 and its graphical interface TmoleX. In all cases, calculations were made at the BP86/TZVP computational level using the solvent effect (COSMO continuum solvation method). In all cases, the independent counter ion (C + A) model was used to describe the ILs. Once the molecules are completely optimized, a single point calculation was carried out in order to ensure that no negative vibrational frequencies are found. Then, all the information required for COSMO-RS calculations is stored in a *.cosmo file, obtained by a single point calculation. COSMOtherm program package (version 19) with its implicit parametrization BP_TZVP_19 was used for COSMO-RS calculations. Henry's law constant and excess property (enthalpy with contributions, entropy, and Gibbs energy) calculations were made for all the systems including the two F-gases and all the IL database. Henry's law constants were calculated by the following equation

$$K_H = \gamma_i^{\infty} \cdot P_0^{vap} \quad (1)$$

where K_H is the Henry's law constant, γ_i^{∞} is the activity coefficient of the solute at infinite dilution in the IL (calculated by COSMOtherm), and P_0^{vap} is the solute vapor pressure estimated by using the Antoine equation (R-134a and R-32 data from literature[52,53]).

https://doi.org/10.1021/acs.est.2c00051
Environ. Sci. Technol. 2022, 56, 5898−5909

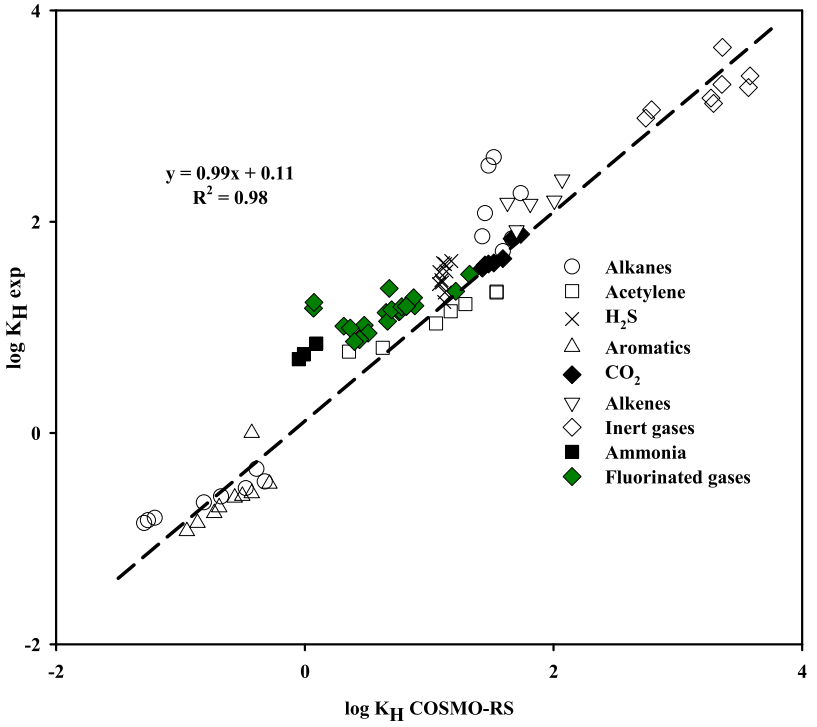

Figure 1. Validation of Henry's law constants (bar) of solutes in ILs, calculated by COSMO-RS determined using experimental vapor pressure of the different solutes at room temperature with C + A model.

2.2. Materials. The ionic liquids and gases used in this work are listed in Table S1 of Supporting Information. The ionic liquid tributyl(ethyl)phosphonium diethyl phosphate, ($[P_{2444}][C_2C_2PO_4]$, >95% mass fraction purity) was supplied by Solvay (Lyon, France), and the ionic liquid trihexyl-(tetradecyl)phosphonium glycinate, ($[P_{66614}][C_2NO_2]$, >95% mass fraction purity) was supplied by Iolitec (Heilbronn, Germany). The ionic liquid trihexyl(tetradecyl)phosphonium 2-cyano-pyrrolide ($[P_{66614}][CNPyr]$, >95% mass fraction purity) was synthetized in our laboratory following the methodology described elsewhere.[54,55] Two solutions of trihexyl(tetradecyl)phosphonium bromide (1.1 g, 2 mmol) in ethanol (200 mL) and Amberlite IRN78 (10 g) were mixed for 2 days using two 500 mL containers. $AgNO_3$ was used to ensure that no residual halide was still present in the mixture, confirming the formation of trihexyl(tetradecyl)phosphonium hydroxide. Then, the solutions were filtered and mixed with pyrrole-2-carbonitrile (0.34 mL, 4 mmol) for 2 days. The volatile compounds were completely removed at 343 K and vacuum pressure (48 Pa). The compounds and materials used for synthesis were supplied by Sigma-Aldrich (Darmstadt, Germany): trihexyl(tetradecyl)phosphonium bromide (>95% mass fraction purity), ethanol (>99% mass fraction purity), Amberlite IRN78 (>95% mass fraction purity), $AgNO_3$ (>99% mass fraction purity), and pyrrole-2-carbonitrile (>95% mass fraction purity). ^1H nuclear magnetic resonance (NMR) spectroscopy was employed to verify the structure of the IL synthesized by using a Bruker Varian Unity 500.

All ILs were dried under vacuum (4 Pa) and vigorously stirred at 323.15 K for at least 48 h, immediately before their use. Difluoromethane (R-32, ≥99.8% mass fraction purity) and 1,1,1,2-tetrafluoroethane (R-134a, ≥ 99.8% mass fraction purity) were acquired from Polo Zero (Lisbon, Portugal) for volumetric measurements and from Euro Refrigerant for gravimetric measurements. Tables S2 and S3 of Supporting Information show the physical properties and degradation temperatures, respectively, of the ILs used in this work. The physical properties were compared and are plotted in Figure S1 of Supporting Information. The thermal stability of ionic liquids is a very important parameter for the application of these compounds. Phosphonium ILs are reported to exhibit higher chemical stability than imidazolium-based ILs.[56,57] Furthermore, the thermal stabilities of $[P_{2444}][C_2C_2PO_4]$, $[P_{66614}][C_2NO_2]$, and $[P_{66614}][CNPyr]$ are reported to be above 580 K (see Table S3 of Supporting Information), showing high degradation temperatures.

2.3. Absorption of F-Gas Measurements. The R-32 and R-134a absorption isotherms in the chosen ILs were determined using an isochoric saturation method at different temperatures (303.15, 313.15, and 323.15 K) and a pressure range of 0.05−0.5 MPa. A certain known amount of gas was put in contact with a precisely quantity of degassed ILs in a completely closed cell, at constant temperature. The equipment contained two subsystems whose respective volume is known and which are interconnected by a needle valve. The first subsystem consisted of a gas tank (stainless steel cylinder) and a LEX 1 manometer (Keller AG, Winterthur, Switzerland) with an accuracy of 0.05% of full scale (FS) in the range of 0.01−2 MPa that allowed us to measure the pressure of this subsystem. The second subsystem comprised an equilibrium cell (stainless-steed cell with a magnetic stirrer) and the pressure of this subsystem was measured with a LEO 2 manometer (Keller AG, Winterthur, Switzerland) with an accuracy of 0.1% FS in a range of 0.01−1 MPa. In order to maintain the isothermal conditions of the equipment, it was immersed in a water bath in which the temperature was controlled with a CORIO CD heating immersion circulator (±0.03 K) from Julabo GmbH (Germany). A Pt100 probe coupled to a Yokogawa 7561 digital multimeter (within ±0.02 K) was used to measure the temperature. The experimental

https://doi.org/10.1021/acs.est.2c00051
Environ. Sci. Technol. 2022, 56, 5898−5909

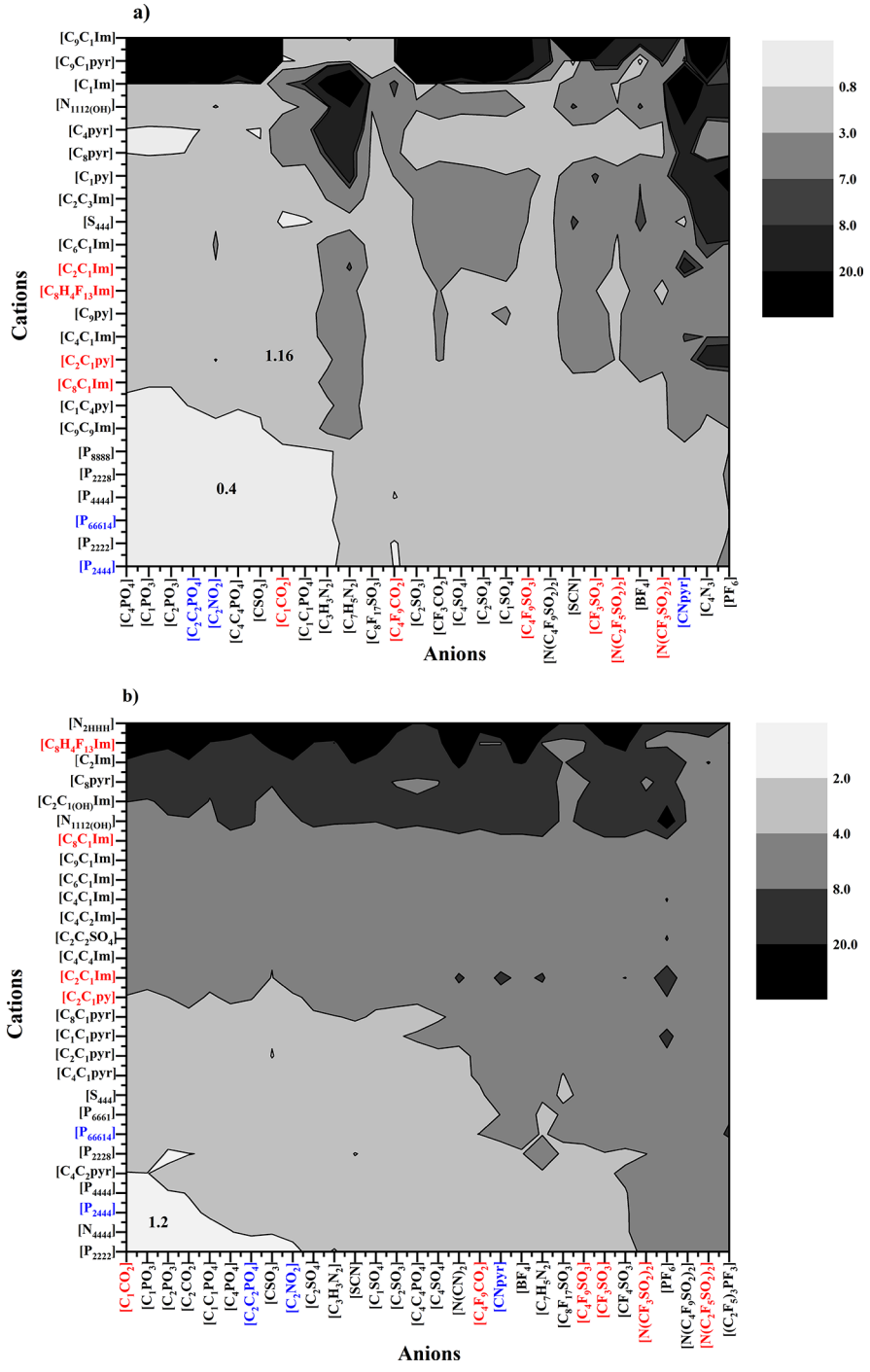

Figure 2. Henry's law constants (bar) screening of (a) R-134a and (b) R-32 in >600 different ILs at T = 298 K calculated by the COSMO-RS method. The blue color highlights the cations and anions studied in this work and the red color highlights the ILs studied in our previous works.[29,30]

setup is depicted in Figure S2 in Supporting Information. More details related to the experimental procedure are explained in Supporting Information (Methods section).

The validation of this experimental method was carried out with the pure IL $[P_{2444}][C_2C_2PO_4]$ for the absorption of R-134a at 303.15 and 323.15 K. Then, the results obtained using the volumetric method were compared with the data measured using the gravimetric method (see Figure S3 of Supporting Information and Tables S4−S7 of Supporting Information), which were measured as a function of pressure and temperature using an Intelligent Gravimetric Analyzer (IGA001) from Hiden Analytical following a procedure previously described.[28,58] In the gravimetric measurements, the pure IL was loaded into the IGA001 sample holder, approximately 70 mg, degassed, and dried during 24 h by a turbo pump (Edwards, EXT75DX) at 303 K before starting the absorption/desorption cycles at each temperature. The detailed measurement setup and data treatment are described in Supporting Information (Methods section) and in our previous work.[58]

The experimental measurements were repeated several times under the same conditions to verify the reproducibility of the

https://doi.org/10.1021/acs.est.2c00051
Environ. Sci. Technol. 2022, 56, 5898−5909

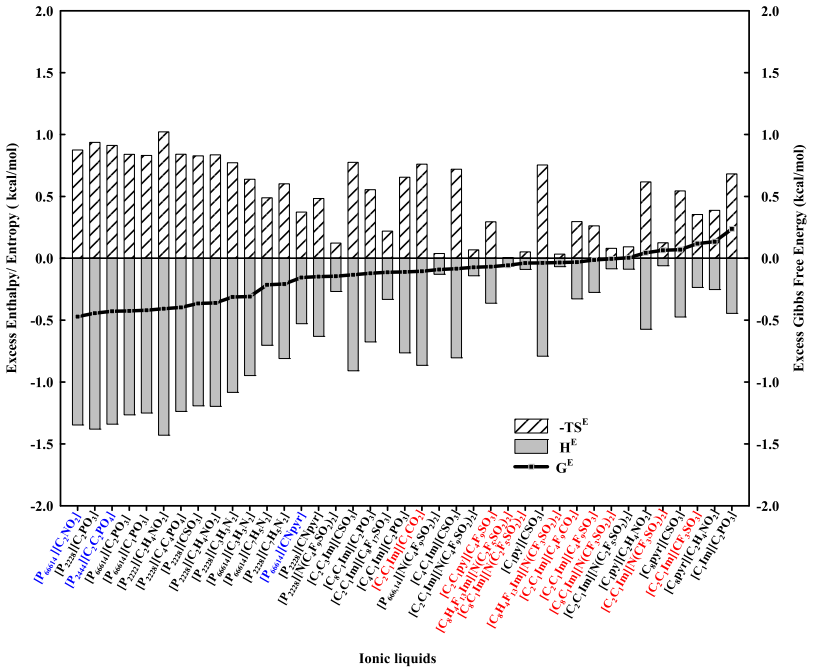

Figure 3. Effect of cations on the excess enthalpy, entropy, and Gibbs free energy of R-134a + IL equimolar mixture calculated using COSMO-RS at T = 298 K. The blue color highlights the cations and anions studied in this work, and the red color highlights the ILs studied in our previous work.[29,30]

data. The overall experimental uncertainty was found to be less than 3%.

3. RESULTS

3.1. Henry's Law Constant Validation. The first step when applying the multiscale research strategy is to validate the predictions made with the COSMO-RS method. In this work, the absorption of F-gases in ILs is evaluated, using Henry's law constant (K_H) as a key parameter of reference for solvent selection. Figure 1 (data reported also in Table S8 of Supporting Information) compares the experimental K_H as a function of calculated K_H for a wide collection of solutes and ILs, including those of very different natures such as inert gases, CO_2, hydrocarbons, among others.

It can be seen that the experimental−computational data follow a general linear trend for all the solutes. Specifically, F-gases (marked in green) are placed in the middle of the trend (in general, higher solubility than CO_2 but lower than NH_3) and following the same linear behavior compared to the rest of the solute's data. Therefore, we can conclude that COSMO-RS predicts reasonably well the experimental K_H trends for a diversity of solutes and ILs with remarkably different chemical natures, including the F-gases of interest in this study. Once COSMO-RS is validated, the next stage is to perform a K_H screening among a representative database of cations and anions (including those that were previously experimentally studied) trying to find some combinations that may improve the performance of those previously presented in the literature. Figure 2a,b presents the results of K_H screening (more than 600 cation/anion combinations) for R-134a and R-32 gases at 298 K, with the cations and anions experimentally studied previously in the literature represented in red and those studied in this work represented in blue. Detailed nomenclature of ILs studied in this work is shown in Table S9 of Supporting Information.

As can be seen in Figure 2a, the K_H values for R-134a solute in ILs present a wide range of values. This means that the proper selection of the IL is important because the gas solubility of R-134a may increase 2 orders of magnitude by choosing adequate cation/anion combination. It can be observed that the selection of both the anion and the cation is important to obtain a low K_H value (high absorption capacity). Analyzing the anions previously studied in the literature (marked in red), we conclude that ILs based on fluorinated carboxylate and sulfonate anions promote intermediate/high R-134a solubility. However, there will appear some anions containing phosphate ($[C_2C_2PO_4]$) or amino acid ($[C_2NO_2]$) groups (marked in blue in Figure 2a) that form ILs with remarkable lower K_H than those previously studied. On the other hand, [CNPyr] anion may be interesting for practical applications in GHG capture because [CNPyr]-based ILs simultaneously behave as the CO_2 chemical absorbent and present high F-gas solubility.[59] Regarding the cation role, it is again found that those cations, previously evaluated (marked in red in Figure 2a), as imidazolium and pyridinium, constitute ILs with intermediate K_H values. Therefore, the correct selection of the cation may significantly improve the solubility of R-134a in the IL. Specifically, it is found that those cations using phosphonium as the head group, as $[P_{66614}]$ and $[P_{2444}]$ (marked in blue in Figure 2a), seem to be the best for the task. Based on the abovementioned results, we select three available ILs ($[P_{2444}][C_2C_2PO_4]$, $[P_{66614}][C_2NO_2]$, and $[P_{66614}]$-[CNPyr])—previously synthesized in our laboratory[54,55]—as promising new R-134a absorbents in F-gas capture for next stages of this work. Figure 2b shows the same COSMO-RS screening of K_H for R-32 solute in >600 ILs. In general, K_H values of R-32 in ILs are slightly higher than that of R-134a, in good agreement with the slightly lower experimental gas solubility reported previously.[20,30] Again, both the cation and the anion are important for the proper selection of the IL. Most of the ILs previously studied (marked in red in Figure

https://doi.org/10.1021/acs.est.2c00051
Environ. Sci. Technol. 2022, 56, 5898−5909

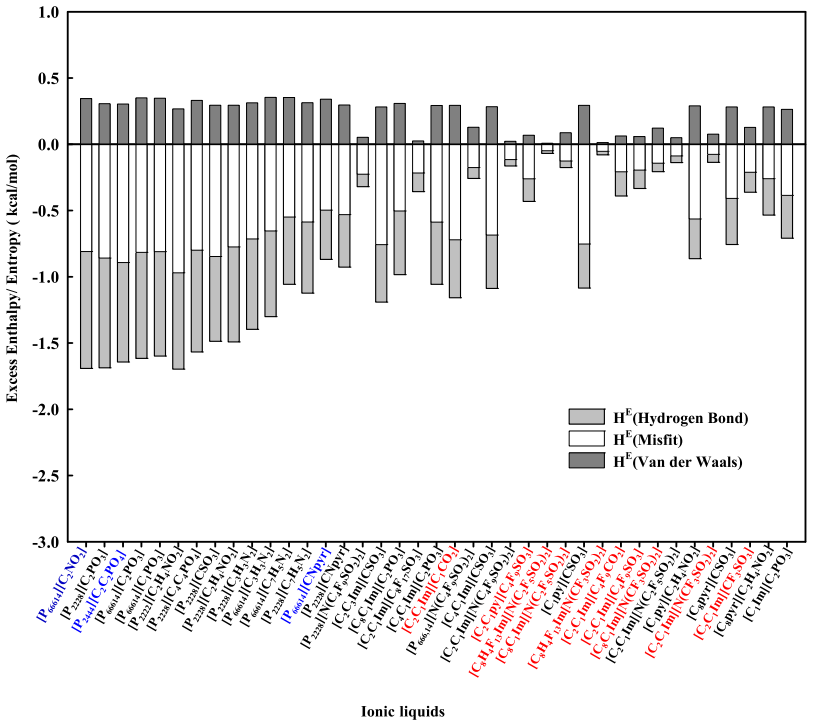

Figure 4. Intermolecular interaction (misfit-electrostatic, van der Waals, and hydrogen-bonding) contributions to excess molar enthalpies of R-134a + IL equimolar mixtures calculated using COSMO-RS (C+ A model). The blue color highlights the cations and anions studied in this work, and the red color highlights the ILs studied in our previous work.[29,30]

2b) are in the range of intermediate/high K_H, implying that some other ILs may offer higher R-32 solubility. It is observed that the selected ILs ($[P_{2444}][C_2C_2PO_4]$, $[P_{66614}][C_2NO_2]$, and $[P_{66614}][CNPyr]$) that are mentioned above seem to be also potential good candidates for R-32 absorption in F-gas treatment. Of course, there are also other interesting combinations (as those including phosphonium cation and $[C_1CO_2]$ anion), but these ILs are not currently available. Therefore, we propose to carry out the subsequent absorption measurements with the available ILs $[P_{2444}][C_2C_2PO_4]$, $[P_{66614}][C_2NO_2]$, and $[P_{66614}][CNPyr]$, as alternative candidates for R-134a and R-32 capture.

COSMO-RS analysis is now used to gain a better fundamental understanding of the thermodynamic of F-gas absorption phenomena in ILs. To do so, the excess properties of the solute−solvent equimolar mixtures were observed. Figures 3 and S4 of Supporting Information show the excess enthalpy, entropy, and Gibbs energy of a representative sample of F-gases + IL mixtures (Figure 3: results for R-134a; Figure S4: results for R-32), involving previously studied ILs (marked in red) and selected ILs (marked in blue). The two figures show that mixtures with previously studied ILs and F-gases promote excess Gibbs energy close to zero, indicating that the absorption of R-134a or R-32 in ILs is not particularly favored thermodynamically. This is directly attributed to the unfavorable entropic contribution to the mixture, despite their exothermic behavior. In contrast, mixtures with the selected ILs and R-134a or R-32 compounds present remarkably more negative excess Gibbs energies, suggesting a more spontaneous absorption process. In these cases, the exothermic enthalpy contribution determines the thermodynamics of the mixture, with the entropy playing a minor role. Clearly, ILs constituted by phosphonium-based cations and anions with phosphate or amino acid-based groups are among those presenting the most spontaneous mixtures with the R-134a refrigerant, in good agreement with the low K_H values found in the abovementioned COSMO-RS screening. Regarding the R-32 compound, the selected ILs are also expected to behave as good absorbents due to the favorable solute−solvent mixture, probably with lower selectivity than R-134a according to the obtained excess properties (less negative G^E values, due to more positive $-TS^E$ term).

We demonstrated that the enthalpic contribution governs the F-gases/IL mixtures in those ILs presenting the most thermodynamically favored absorption process, and Figures 4 and S5 of Supporting Information show the detailed contributions of the intermolecular interactions to the excess enthalpy in the equimolar mixtures of F-gases/ILs where Figure 4 shows the results for R-134a and Figure S5 of Supporting Information for R-32. The intermolecular interactions in the liquid are calculated following the equation

$$H^E = H^E(\mathrm{HB}) + H^E(\mathrm{MF}) + H^E(\mathrm{vdW}) \quad (2)$$

where H^E is the excess enthalpy, and it is obtained by the sum of hydrogen bonding (HB), electrostatic-misfit (MF), and van der Waals (vdW) contributions.

Figures 4 and S5 of Supporting Information show that attractive hydrogen bonding and electrostatic intermolecular interactions between R-134a and R-32 and IL components are responsible of the exothermic enthalpy of these mixtures. On the contrary, van der Waals contributions are unfavorable to the mixing phenomena. Paying special attention to the differences between the ILs previously studied (marked in red) and the new proposed ILs (marked in blue), one main difference is the anion nature. The most promising anions are those presenting remarkable polar structures with oxygenated or nitrogenated functional groups, able to behave as hydrogen bond acceptor groups. This promotes attractive electrostatic

https://doi.org/10.1021/acs.est.2c00051
Environ. Sci. Technol. 2022, 56, 5898−5909

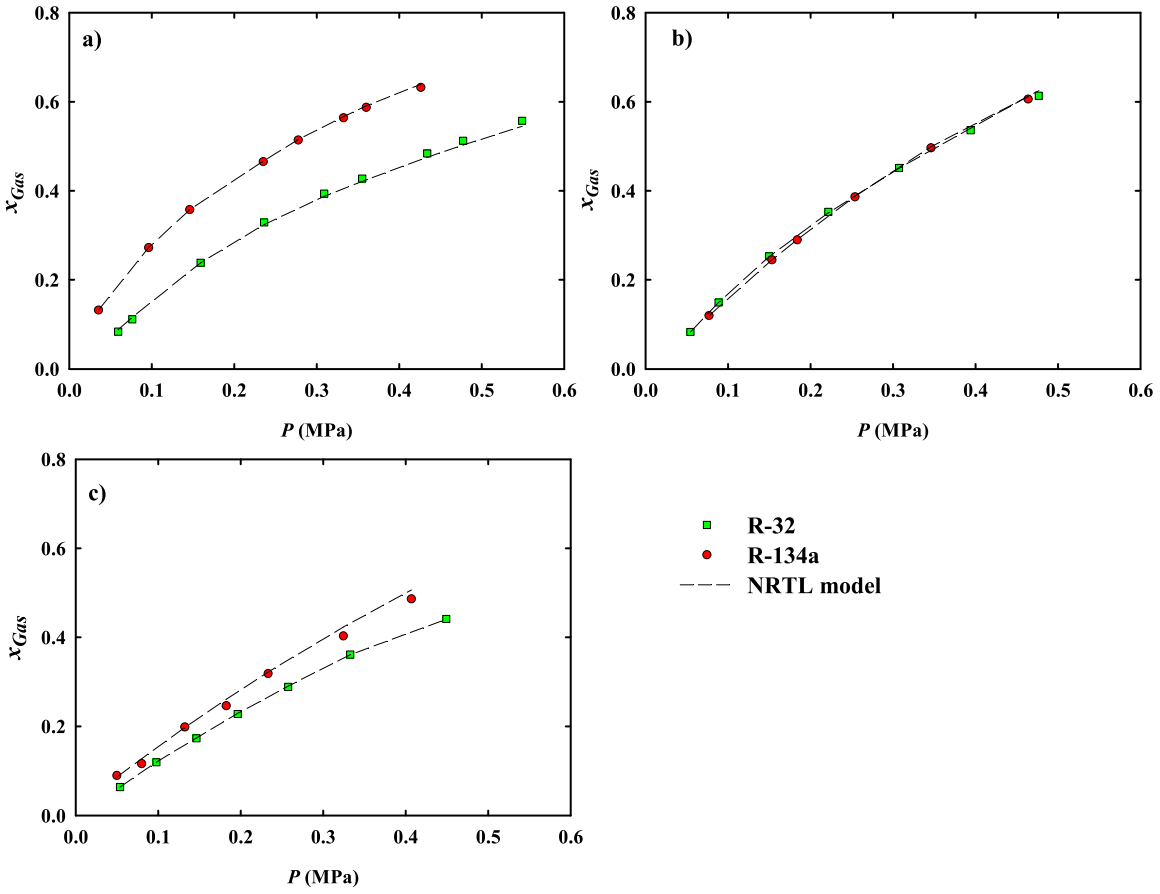

Figure 5. Absorption equilibrium isotherms of F-gas in: (a) $[P_{2444}][C_2C_2PO_4]$; (b) $[P_{66614}][C_2NO_2]$; and (c) $[P_{66614}][CNPyr]$ at 303.15 K. The dashed lines represent the fitting using the NRTL model.

interactions and hydrogen bonds with R-134a and R-32 molecules, which present a weak acidic character.[60] Regarding the cation, ILs marked in red are based on the imidazolium cation, whereas ILs marked in blue include phosphonium-based cations. Imidazolium are polar structures presenting hydrogen bond donor groups, promoting strong anion−cation interactions. In contrast, phosphonium-based cations are nearly nonpolar structures due to their long alkyl chains, with low capacity to form hydrogen bonds. As a consequence, designing ILs based on the phosphonium cation and basic anion promote effective F-gas solute—IL solvent interaction, avoiding competitive effects due to cation−anion interaction. Summarizing that COSMO-RS computational analysis indicates that the three selected IL should have a better performance (in the order of $[P_{2444}][C_2C_2PO_4]$ > $[P_{66614}][C_2NO_2]$ > $[P_{66614}][CNPyr]$) for R-134a and R-32 absorption than other previously studied ILs.

3.2. Determination of Gas Absorption. Previous works showed that the solubility of F-gas in F-ILs is determined by the affinity between the fluorinated moieties of the solutes and the solvents.[61−64] The nature of the C−F bonds in the FILs are marked by the high electronegativity of fluorine, enhancing the absorption of F-gases.[65,66] All these properties motivated us to evaluate FILs in process simulation,[20] where we demonstrated the practical limitations of these compounds due to their high viscosities and high molar weights.[20]

In this work, a COSMO-RS mapping was performed using the Henry's constants between F-gas with approximately 600 ILs in order to understand the thermodynamic behavior and interactions that improve and enhance the solute/solvent interactions in the F-gas + IL systems. Then, three ILs were selected to improve the physical absorption of F-gas, taking into account different criteria such as Henry's constant and molecular interactions like hydrogen-bonding, electrostatic, and van der Waals.[45] We, thus, provide an alternative route to FILs or conventional solvents for F-gas capture. The three selected ILs were evaluated using gravimetric and volumetric methods.

The experimental solubility data are shown in Figures 5 and S6−S7 of Supporting Information, expressed as mole fraction of the solubilized F-gas in the three ILs. The isotherms were measured at temperatures from 303.15 to 323.15 K and in a range of equilibrium pressures from 0.5 to 5.5 MPa for the F-gases under study (see also Tables S4−S7 of Supporting Information). The maximum equilibrium pressures are selected 80% below the saturation pressure of F-gas in order to be uniform in all experimental data. The experimental isotherms were correlated using the NRTL thermodynamic model (see all information in Supporting Information).

For quantitative comparison, Table S12 of Supporting Information shows the F-gas solubility in currently and previously studied ILs at 303.15 K and 0.1, 0.2, and 0.4 MPa using molar (x) and mass (w) units. The experimental absorption isotherms show that the mole fraction solubility increases in the order $[P_{66614}][CNPyr] < [P_{66614}][C_2NO_2] \leq [P_{2444}][C_2C_2PO_4]$ for R-134a and R-32, in good agreement with COSMO-RS predictions, with the absorption being higher at lower temperatures, as expected. R-32 has one less

https://doi.org/10.1021/acs.est.2c00051
Environ. Sci. Technol. 2022, 56, 5898−5909

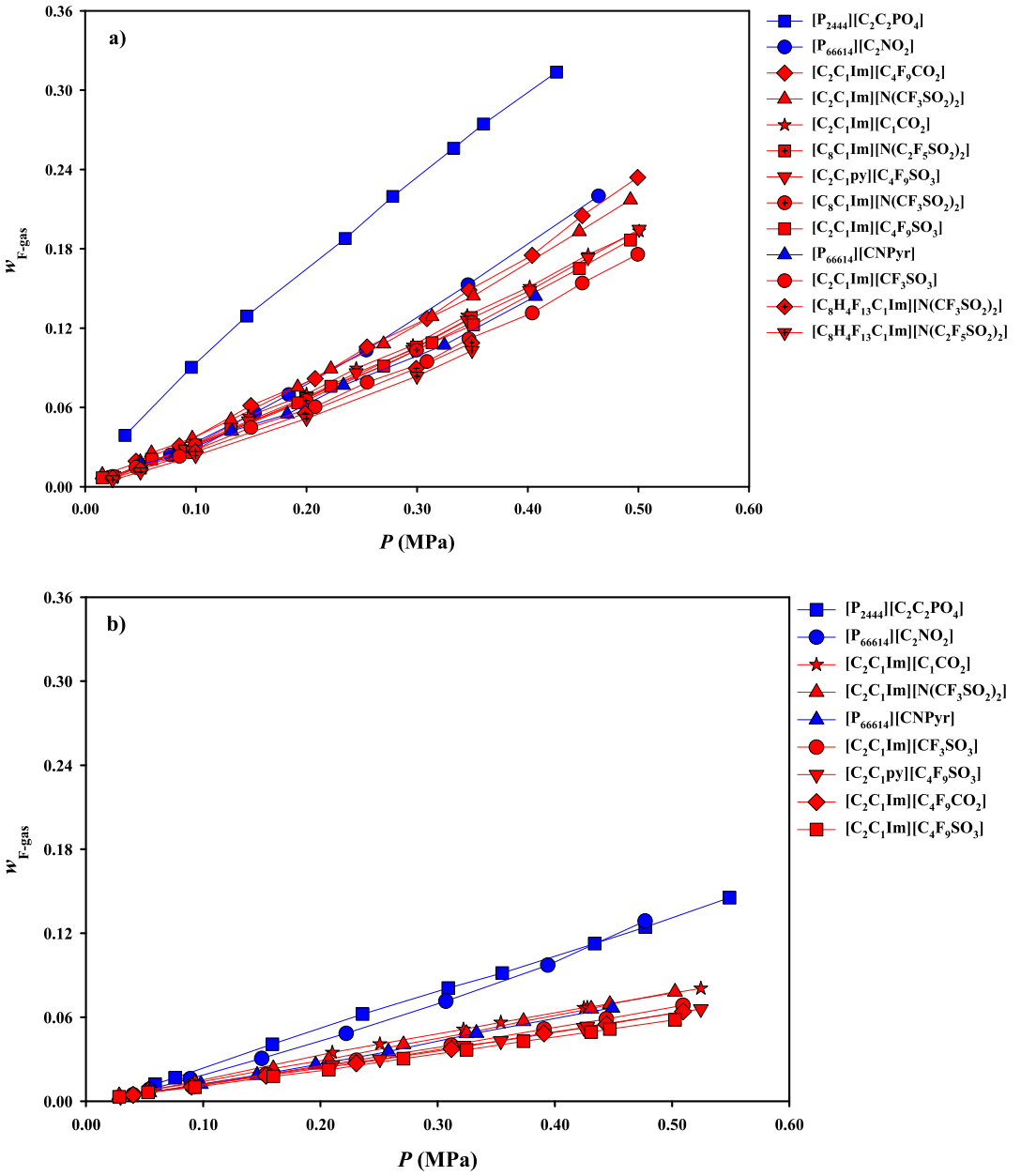

Figure 6. Comparison of the absorption equilibrium isotherms, in mass fraction unit, for the F-gas in ILs of this work ($[P_{2444}][C_2C_2PO_4]$, $[P_{66614}][C_2NO_2]$, and $[P_{66614}][CN_{Pyr}]$) and ILs studied in our previous work[29,30] at 303.15 K where (a) R-134a and (b) R-32.

fluorine atom and lower hydrogen bonding capacity, directly affecting the solubility in all ILs studied in this work except for $[P_{66614}][C_2NO_2]$ where similar values are obtained for R-32 and R-134a. Figure 6 shows the comparison of the experimental F-gas solubility data in mass fraction of the ILs studied in this work with those reported in the literature,[29,30] because mass unit is more commonly used in the industrial process.[37,67] As can be seen, the selected IL $[P_{2444}][C_2C_2PO_4]$ presents remarkably enhanced R-134a and R-32 absorption mass capacity compared to previously studied ILs and FILs, a fact that could be attributed to more favorable solute−solvent interactions as well as to the molar weight of $[P_{2444}][C_2C_2PO_4]$. $[P_{66614}][C_2NO_2]$ also presents a relatively high mass solubility, better or similar the values reported for FILs or other ILs in the literature, demonstrating that F-gas solubility can be enhanced by hydrogen bond acceptor ILs as the ones selected in this work or by hydrogen bond donor ILs as the FILs studied previously. As expected from COSMO-RS calculations, the CO_2 chemical absorbent $[P_{66614}][CNPyr]$ presents a reasonably high mass uptake of R-134a and R-32 gases, close to those previously reported for FILs, making this IL an interesting absorbent for combined greenhouse gases treatments.

In addition, Henry's constants were determined from the experimental gas absorption data in order to complete current computational−experimental analysis. Henry's constant, K_H,[26,27,54] for component i is defined as

$$K_{Hi} = \lim_{x_i \to 0} \frac{\phi_i(P,\ T)P}{x_i} \tag{3}$$

where x_i is the mole fraction of F-gas dissolved in ILs, P is the equilibrium pressure, and ϕ_i refers to the fugacity of F-gas. The Henry's constants were determined for experimental and

https://doi.org/10.1021/acs.est.2c00051
Environ. Sci. Technol. 2022, 56, 5898−5909

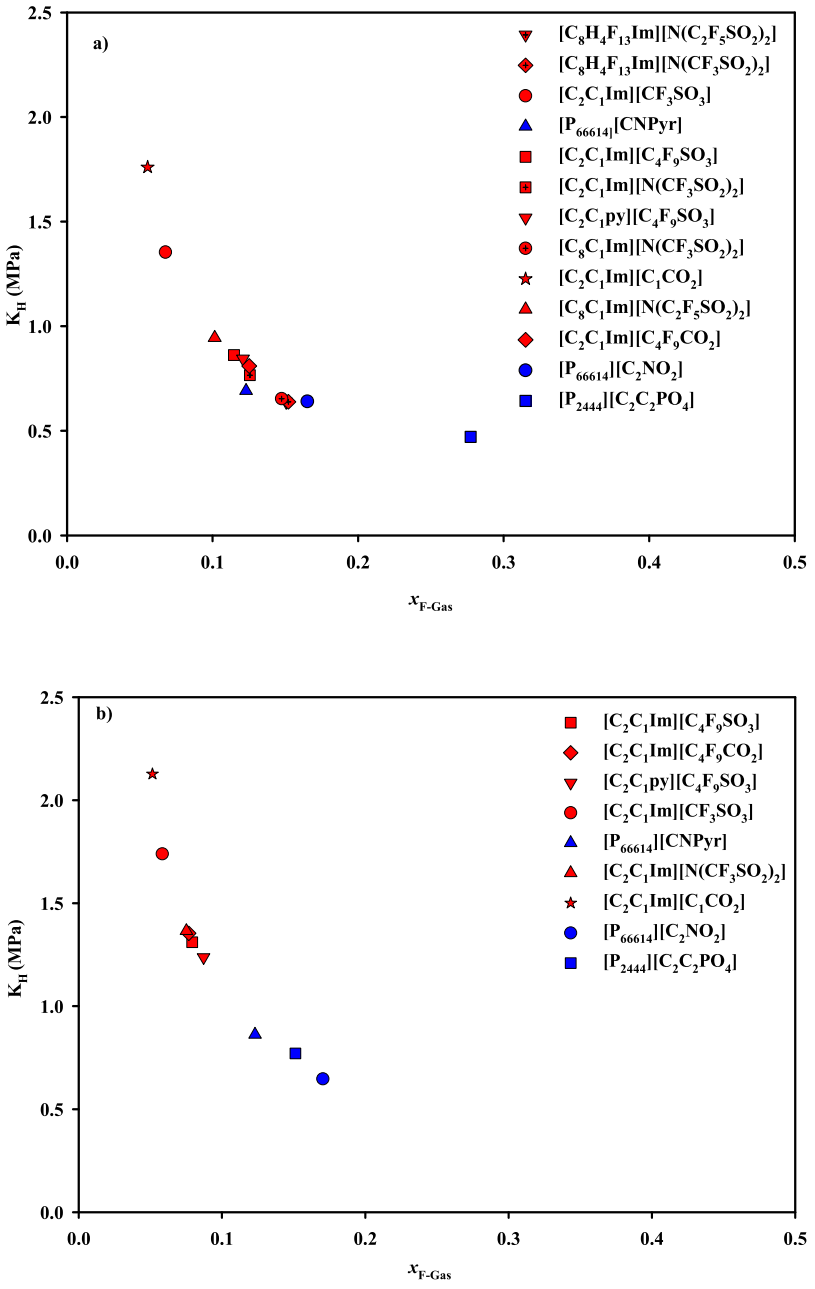

Figure 7. Comparison of Henry constants vs mass solubility the F-gas in ILs studied in this work ($[P_{2444}][C_2C_2PO_4]$, $[P_{66614}][C_2NO_2]$, and $[P_{66614}][CNPyr]$) and ILs studied in our previous work[29,30] at 303.15 K and 0.1 MPa where: (a) R-134a and (b) R-32.

literature data[29,30] and are shown in Table S12 of Supporting Information. Figure 7 shows the comparison of the experimentally obtained Henry's constant with the molar fraction of R-134a and R-32 in selected ILs (this work) and previously studied FILs or ILs. Figure 7 clearly shows the excellent thermodynamic behavior of $[P_{2444}][C_2C_2PO_4]$, particularly for R-134a absorption, whereas the other two selected ILs, $[P_{66614}][CNPyr]$ and $[P_{66614}][C_2NO_2]$, also present favorable absorption capacities. It should be remarked the high R-32/R-134a selectivity (see also Figure S8 of Supporting Information) of proposed ILs what could be taken advantage for potential separation of F-gas-based refrigerants.

The selected ILs compare favorably as F-gas absorbents but because their viscosity (see Table S2 of Supporting Information) is higher than that of the FILs previously proposed,[20] more research has to be conducted to evaluate the process performance of $[P_{2444}][C_2C_2PO_4]$, $[P_{66614}][C_2NO_2]$, and $[P_{66614}][CNPyr]$ in commercial industrial equipment. Furthermore, toxicity studies are very important for the industrial application of these compounds and will also have to be carried out to complete the characterization of these compounds.

In this work, a thermodynamic analysis of the solubility of the F-gases (R-134a and R-32) in ILs was performed by means of the COSMO-RS method. This study allows us to explore different cations and anions, combined in approximately 600 ILs, and to select three with a significantly improved solubility with respect to those reported in the literature. Henry's constant was the descriptor used to select the ILs because this thermodynamic benchmark quantity probes solute−solvent interactions. The selected ILs present significantly more negative excess Gibbs free energy when mixed with the F-

https://doi.org/10.1021/acs.est.2c00051
Environ. Sci. Technol. 2022, 56, 5898−5909

gases and contribute to a more spontaneous absorption process. The hydrogen bond acceptor character of the IL anions plays an important role in favorable solute−solvent interactions. Experimental measurements confirmed COSMO-RS predictions with $[P_{2444}][C_2C_2PO_4]$, presenting a higher R-134a and R-32 absorption capacity than any other IL previously studied, whereas selected $[P_{66614}][C_2NO_2]$ and $[P_{66614}][CNPyr]$ may be just competitive solvent alternatives in the F-gas absorption process.

■ ASSOCIATED CONTENT

Supporting Information

The Supporting Information is available free of charge at https://pubs.acs.org/doi/10.1021/acs.est.2c00051.

Chemical structures and acronyms of the ILs, physical properties of the ILs, degradation temperature of ILs, experimental setup, comparison of experimental absorption data, molar absorption fraction, experimental and COSMO-RS Henry's law constants of solutes in ILs, cations and anions of the ILs, effect of cation on the excess enthalpy, entropy, and Gibbs free energy, intermolecular interaction (misfit-electrostatic, van der Waals, and hydrogen-bonding) contributions, absorption equilibrium isotherms, NRTL parameters, comparison of the molar (x) and mass (w) solubility and Henry's constant for the F-gas in ILs, and ideal selectivity at 303.15 K, determined from the Henry's constants, for the ILs (PDF)

■ AUTHOR INFORMATION

Corresponding Authors

José Palomar − *Chemical Engineering Department, Universidad Autónoma de Madrid, Madrid 28049, Spain;* orcid.org/0000-0003-4304-0515; Email: pepe.palomar@uam.es

Ana B. Pereiro − *LAQV, REQUIMTE, Department of Chemistry, NOVA School of Science and Technology, NOVA University Lisbon, Caparica 2829-516, Portugal;* orcid.org/0000-0001-7166-6764; Email: anab@fct.unl.pt

Authors

Julio E. Sosa − *LAQV, REQUIMTE, Department of Chemistry, NOVA School of Science and Technology, NOVA University Lisbon, Caparica 2829-516, Portugal*

Rubén Santiago − *Chemical Engineering Department, Universidad Autónoma de Madrid, Madrid 28049, Spain;* orcid.org/0000-0002-6877-9001

Andres E. Redondo − *LAQV, REQUIMTE, Department of Chemistry, NOVA School of Science and Technology, NOVA University Lisbon, Caparica 2829-516, Portugal*

Jocasta Avila − *Laboratoire de Chimie, École Normale Superieure de Lyon & CNRS, Lyon 69364, France*

Luiz F. Lepre − *Laboratoire de Chimie, École Normale Superieure de Lyon & CNRS, Lyon 69364, France;* orcid.org/0000-0003-4566-7063

Margarida Costa Gomes − *Laboratoire de Chimie, École Normale Superieure de Lyon & CNRS, Lyon 69364, France;* orcid.org/0000-0001-8637-6057

João M. M. Araújo − *LAQV, REQUIMTE, Department of Chemistry, NOVA School of Science and Technology, NOVA University Lisbon, Caparica 2829-516, Portugal;* orcid.org/0000-0002-8648-7539

Complete contact information is available at: https://pubs.acs.org/10.1021/acs.est.2c00051

Author Contributions

The manuscript was designed and written through contributions of all authors. All authors have given approval to the final version of the manuscript.

Funding

This work was also supported by Associate Laboratory for Green Chemistry−LAQV, financed by national funds from FCT/MCTES (UID/QUI/50006/2020), the contracts of Individual Call to Scientific Employment Stimulus 2020.00835.CEECIND (J.M.M.A.)/2021.01432.CEECIND (A.B.P.) and by FCT/MCTES (Portugal) through the project PTDC/EQU-EQU/29737/2017. The authors thank Solvay for providing the ionic liquid tri(butyl) ethylphosphonium diethylphosphate. M.C.G. and J.A. thank IDEX-LYON for financial support (Programme Investissement d'Avenir ANR-16-IDEX-0005).

Notes

The authors declare no competing financial interest.

■ REFERENCES

(1) European Environment Agency. Fluorinated Greenhouse Gases | Climate Action. https://www.eea.europa.eu/data-and-maps/indicators/emissions-and-consumption-of-fluorinated-2/assessment-2 (accessed on 23 August 2021).

(2) European Environment Agency (EEA). Emissions and Supply of Fluorinated Greenhouse Gases in Europe. Available online. https://www.eea.europa.eu/data-and-maps/indicators/emissions-and-consumption-of-fluorinated-2/assessment-2 (accessed on 21 August 2021).

(3) Wang, Z.; Wang, Y.; Li, J.; Henne, S.; Zhang, B.; Hu, J.; Zhang, J. Impacts of the Degradation of 2,3,3,3-Tetrafluoropropene into Trifluoroacetic Acid from Its Application in Automobile Air Conditioners in China, the United States, and Europe. *Environ. Sci. Technol.* **2018**, *52*, 2819−2826.

(4) Professional Waste Irregular Management of Refrigerators Reported in Several European CountriesAvailable online: https://www.residuosprofesional.com/gestion-irregular-refrigeradores-paises/ (accessed on 21 August 2021).

(5) Eskander, S. M. S. U.; Fankhauser, S. Reduction in Greenhouse Gas Emissions from National Climate Legislation. *Nat. Clim. Change* **2020**, *10*, 750−756.

(6) Rhoads, A.; Hill, W. Development of a Tool for Estimating the Life Cycle Climate Performance of MAC Systems. *SAE [Tech. Pap.]* **2019**, *2019*, 7666−7672.

(7) Keri, C. Recycling Cooling and Freezing Appliances. *Waste Electrical and Electronic Equipment (WEEE) Handbook*; Elsevier Science, 2012; pp 339−351.

(8) Wang, Q.; Wang, X.; Ding, X. Rainwater Trifluoroacetic Acid (TFA) in Guangzhou, South China: Levels, Wet Deposition Fluxes and Source Implication. *Sci. Total Environ.* **2014**, *468*−*469*, 272−279.

(9) Boutonnet, J. C.; Bingham, P.; Calamari, D.; de Rooij, C.; Franklin, J.; Kawano, T.; Libre, J.-M.; McCul-loch, A.; Malinverno, G.; Odom, J. M.; et al. Environmental Risk Assessment of Trifluoroacetic Acid. *Hum. Ecol. Risk Assess.* **1999**, *5*, 59−124.

(10) Scott, B. F.; Spencer, C.; Martin, J. W.; Barra, R.; Bootsma, H. A.; Jones, K. C.; Johnston, A. E.; Muir, D. C. G. Comparison of Haloacetic Acids in the Environment of the Northern and Southern Hemispheres. *Environ. Sci. Technol.* **2005**, *39*, 8664−8670.

(11) Hanson, M. L.; Sibley, P. K.; Mabury, S. A.; Solomon, K. R.; Muir, D. C. G. Trichloroacetic Acid (TCA) and Trifluoroacetic Acid (TFA) Mixture Toxicity to the Macrophytes Myriophyllum Spicatum

and Myriophyllum Sibiricum in Aquatic Microcosms. *Sci. Total Environ.* **2002**, *285*, 247−259.
(12) Finlayson-Pitts, B. J.; Pitts, J. N. Global Tropospheric Chemistry and Climate Change. *Chemistry of the upper and lower atmosphere* **2000**, 762−843.
(13) Tsai, W.-T. An Overview of Environmental Hazards and Exposure Risk of Hydrofluorocarbons (HFCs). *Chemosphere* **2005**, *61*, 1539−1547.
(14) Mota-Babiloni, A.; Makhnatch, P.; Khodabandeh, R. Recent investigations in HFCs substitution with lower GWP synthetic alternatives: Focus on energetic performance and environmental impact. *Int. J. Refrig.* **2017**, *82*, 288−301.
(15) Öko-Recherche. Briefing Paper: Availability of alternatives to HFCs in commercial refrigeration in the EUNo Title Available online:accessed. https://www.oekorecherche.de/en/node/205 (December 2021).
(16) Sosa, J. E.; Malheiro, C.; Ribeiro, R. P.; Castro, P. J.; Piñeiro, M. M.; Araújo, J. M.; Plantier, F.; Mota, J. P.; Pereiro, A. B. Adsorption of Fluorinated Greenhouse Gases on Activated Carbons: Evaluation of Their Potential for Gas Separation. *J. Chem. Technol. Biotechnol.* **2020**, *95*, 1892−1905.
(17) Wanigarathna, D. J. A.; Gao, J.; Takanami, T.; Zhang, Q.; Liu, B. Adsorption Separation of R-22, R-32 and R-125 Fluorocarbons Using 4A Molecular Sieve Zeolite. *ChemistrySelect* **2016**, *1*, 3718−3722.
(18) Rogers, R. D.; Seddon, K. R. Ionic Liquids—Solvents of the Future? *Science* **2003**, *302*, 792−793.
(19) Plechkova, N. V.; Seddon, K.R. Applications of Ionic Liquids in the Chemical Industry. *Chem. Soc. Rev.* **2008**, *37*, 123−150.
(20) Sosa, J. E.; Santiago, R.; Hospital-Benito, D.; Costa Gomes, M.; Araújo, J. M. M.; Pereiro, A. B.; Palomar, J. Process Evaluation of Fluorinated Ionic Liquids as F-Gas Absorbents. *Environ. Sci. Technol.* **2020**, *54*, 12784−12794.
(21) Shiflett, M. B.; Yokozeki, A. Solubility and Diffusivity of Hydrofluorocarbons in Room-Temperature Ionic Liquids. *AIChE J.* **2006**, *52*, 1205−1219.
(22) Liu, X.; He, M.; Lv, N.; Qi, X.; Su, C. Vapor−Liquid Equilibrium of Three Hydrofluorocarbons with [HMIM][Tf_2N]. *J. Chem. Eng. Data* **2015**, *60*, 1354−1361.
(23) Ren, W.; Scurto, A. M. Phase Equilibria of Imidazolium Ionic Liquids and the Refrigerant Gas, 1,1,1,2-Tetrafluoroethane (R-134a). *Fluid Phase Equilib.* **2009**, *286*, 1−7.
(24) Shiflett, M. B.; Yokozeki, A. Solubility Differences of Halocarbon Isomers in Ionic Liquid [Emim][Tf_2N]. *J. Chem. Eng. Data* **2007**, *52*, 2007−2015.
(25) Liu, X.; Lv, N.; Su, C.; He, M. Solubilities of R32, R245fa, R227ea and R236fa in a Phosphonium-Based Ionic Liquid. *J. Mol. Liq.* **2016**, *218*, 525−530.
(26) Shiflett, M. B.; Yokozeki, A. Absorption Cycle Utilizing Ionic Liquid As Working Fluid. U.S. Patent. 8,506,839 B2, 2006.
(27) Dong, L.; Zheng, D.; Sun, G.; Wu, X. Vapor-Liquid Equilibrium Measurements of Difluoromethane + [Emim]OTf, Difluoromethane + [Bmim]OTf, Difluoroethane + [Emim]OTf, and Difluoroethane + [Bmim]OTf Systems. *J. Chem. Eng. Data* **2011**, *56*, 3663−3668.
(28) Lepre, L. F.; Szala-Bilnik, J.; Pison, L.; Traïkia, M.; Pádua, A. A. H.; Ando, R. A.; Costa Gomes, M. F. Can the Tricyanomethanide Anion Improve CO_2 Absorption by Acetate-Based Ionic Liquids? *Phys. Chem. Chem. Phys.* **2017**, *19*, 12431−12440.
(29) Lepre, L. F.; Andre, D.; Denis-Quanquin, S.; Gautier, A.; Pádua, A. A. H.; Costa Gomes, M. Ionic Liquids Can Enable the Recycling of Fluorinated Greenhouse Gases. *ACS Sustain. Chem. Eng.* **2019**, *7*, 16900−16906.
(30) Sosa, J. E.; Ribeiro, R. P. P. L.; Castro, P. J.; Mota, J. P. B.; Araújo, J. M. M.; Pereiro, A. B. Absorption of Fluorinated Greenhouse Gases Using Fluorinated Ionic Liquids. *Ind. Eng. Chem. Res.* **2019**, *58*, 20769−20778.
(31) Shiflett, M. B.; Yokozeki, A. Gaseous Absorption of Fluoromethane, Fluoroethane, and 1,1,2,2-Tetrafluoroethane in 1-Butyl-3-Methylimidazolium Hexafluorophosphate. *Ind. Eng. Chem. Res.* **2006**, *45*, 6375−6382.
(32) Jiang, Y.; Lei, Z.; Yu, G. Unraveling Weak Interactions between Fluorinated Gases and Ionic Liquids. *Chem. Eng. Sci.* **2021**, *244*, 116792.
(33) Ferro, V. R.; Moya, C.; Moreno, D.; Santiago, R.; De Riva, J.; Pedrosa, G.; Larriba, M.; Diaz, I.; Palomar, J. Enterprise Ionic Liquids Database (ILUAM) for Use in Aspen ONE Programs Suite with COSMO-Based Property Methods. *Ind. Eng. Chem. Res.* **2018**, *57*, 980−989.
(34) Bedia, J.; Ruiz, E.; de Riva, J.; Ferro, V. R.; Palomar, J.; Rodriguez, J. J. Optimized Ionic Liquids for Toluene Absorption. *AIChE J.* **2013**, *59*, 1648−1656.
(35) Palomar, J.; Gonzalez-Miquel, M.; Bedia, J.; Rodriguez, F.; Rodriguez, J. J. Task-Specific Ionic Liquids for Efficient Ammonia Absorption. *Sep. Purif. Technol.* **2011**, *82*, 43−52.
(36) Klamt, A. COSMO-RS: From Quantum Chemistry to Fluid Phase Thermodynamics. *Comput.-Aided Chem. Eng.* **2018**, *43*, 9.
(37) Palomar, J.; Larriba, M.; Lemus, J.; Moreno, D.; Santiago, R.; Moya, C.; De Riva, J.; Pedrosa, G. Demonstrating the Key Role of Kinetics over Thermodynamics in the Selection of Ionic Liquids for CO_2 Physical Absorption. *Sep. Purif. Technol.* **2019**, *213*, 578−586.
(38) Santiago, R.; Moya, C.; Palomar, J. Siloxanes Capture by Ionic Liquids: Solvent Selection and Process Evaluation. *Chem. Eng. J.* **2020**, *401*, 126078.
(39) Santiago, R.; Bedia, J.; Moreno, D.; Moya, C.; de Riva, J.; Larriba, M.; Palomar, J. Acetylene Absorption by Ionic Liquids: A Multiscale Analysis Based on Molecular and Process Simulation. *Sep. Purif. Technol.* **2018**, *204*, 38−48.
(40) de Riva, J.; Suarez-Reyes, J.; Moreno, D.; Díaz, I.; Ferro, V.; Palomar, J. Ionic Liquids for Post-Combustion CO2 Capture by Physical Absorption: Thermodynamic, Kinetic and Process Analysis. *Int. J. Greenh. Gas Control* **2017**, *61*, 61−70.
(41) Santiago, R.; Lemus, J.; Outomuro, A. X.; Bedia, J.; Palomar, J. Assessment of Ionic Liquids as H2S Physical Absorbents by Thermodynamic and Kinetic Analysis Based on Process Simulation. *Sep. Purif. Technol.* **2020**, *233*, 116050.
(42) Tan, L.; Zhu, J.; Zhou, M.; He, X.; Zhang, S. The Effect of Imidazolium and Phosphonium Ionic Liquids on Toluene Absorption Studied by a Molecular Simulation. *J. Mol. Liq.* **2020**, *298*, 112054.
(43) Moya, C.; Santiago, R.; Hospital-Benito, D.; Lemus, J.; Palomar, J. Design of Biogas Upgrading Processes Based on Ionic Liquids. *Chem. Eng. J.* **2022**, *428*, 132103.
(44) Ruiz, E.; Ferro, V. R.; Palomar, J.; Ortega, J.; Rodriguez, J. J. Interactions of Ionic Liquids and Acetone: Thermodynamic Properties, Quantum-Chemical Calculations, and NMR Analysis. *J. Phys. Chem. B* **2013**, *117*, 7388−7398.
(45) Palomar, J.; Gonzalez-Miquel, M.; Polo, A.; Rodriguez, F. Understanding the Physical Absorption of CO_2 in Ionic Liquids Using the COSMO-RS Method. *Ind. Eng. Chem. Res.* **2011**, *50*, 3452−3463.
(46) Gonzalez-Miquel, M.; Palomar, J.; Rodriguez, F. Selection of Ionic Liquids for Enhancing the Gas Solubility of Volatile Organic Compounds. *J. Phys. Chem. B* **2012**, *117*, 296−306.
(47) Gonzalez-Miquel, M.; Talreja, M.; Ethier, A. L.; Flack, K.; Switzer, J. R.; Biddinger, E. J.; Pollet, P.; Palomar, J.; Rodriguez, F.; Eckert, C. A.; et al. COSMO-RS Studies: Structure-Property Relationships for CO_2 Capture by Reversible Ionic Liquids. *Ind. Eng. Chem. Res.* **2012**, *51*, 16066−16073.
(48) Gonzalez-Miquel, M.; Bedia, J.; Abrusci, C.; Palomar, J.; Rodriguez, F. Anion Effects on Kinetics and Thermodynamics of CO_2 Absorption in Ionic Liquids. *J. Phys. Chem. B* **2013**, *117*, 3398−3406.
(49) Gonzalez-Miquel, M.; Bedia, J.; Palomar, J.; Rodriguez, F. Solubility and Diffusivity of CO_2 in Hxmim NTf_2, Omim NTf_2, and Dcmim NTf_2 at T = (298.15, 308.15, and 323.15) K and Pressures up to 20 Bar. *J. Chem. Eng. Data* **2014**, *59*, 212.
(50) Moya, C.; Palomar, J.; Gonzalez-Miquel, M.; Bedia, J.; Rodriguez, F. Diffusion Coefficients of CO2 in Ionic Liquids Estimated by Gravimetry. *Ind. Eng. Chem. Res.* **2014**, *53*, 13782−13789.

https://doi.org/10.1021/acs.est.2c00051
Environ. Sci. Technol. 2022, 56, 5898−5909

(51) Hospital-Benito, D.; Lemus, J.; Moya, C.; Santiago, R.; Ferro, V. R.; Palomar, J. Techno-Economic Feasibility of Ionic Liquids-Based CO2 Chemical Capture Processes. *Chem. Eng. J.* **2021**, *407*, 127196.
(52) Fujiwara, K.; Nakamura, S.; Noguchi, M. Critical Parameters and Vapor Pressure Measurements for 1,1,1-Trifluoroethane (R-143a). *J. Chem. Eng. Data* **1998**, *43*, 55−59.
(53) Fu, Y.-D.; Han, L.-Z.; Zhu, M.-S. PVT Properties, Vapor Pressures and Critical Parameters of HFC-32. *Fluid Phase Equilib.* **1995**, *111*, 273−286.
(54) Moya, C.; Sabater, V.; Yagüe, G.; Larriba, M.; Palomar, J. CO_2 Conversion to Cyclic Carbonates Catalyzed by Ionic Liquids with Aprotic Heterocyclic Anions: DFT Calculations and Operando FTIR Analysis. *J. CO2 Util.* **2018**, *28*, 66−72.
(55) Santiago, R.; Hernández, E.; Moya, C.; Vela, S.; Navarro, P.; Palomar, J. Fatty Alcohol/Water Reaction-Separation Platform to Produce Propylene Carbonate from Captured CO_2 Using a Hydrophobic Ionic Liquid. *Sep. Purif. Technol.* **2021**, *275*, 119143.
(56) Xue, Z.; Qin, L.; Jiang, J.; Mu, T.; Gao, G. Thermal, Electrochemical and Radiolytic Stabilities of Ionic Liquids. *Phys. Chem. Chem. Phys.* **2018**, *20*, 8382−8402.
(57) Wang, B.; Qin, L.; Mu, T.; Xue, Z.; Gao, G. Are Ionic Liquids Chemically Stable? *Chem. Rev.* **2017**, *117*, 7113−7131.
(58) Avila, J.; Červinka, C.; Dugas, P.-Y.; Pádua, A. A. H.; Costa Gomes, M. Porous Ionic Liquids: Structure, Stability, and Gas Absorption Mechanisms. *Adv. Mater. Interfaces* **2021**, *8*, 2001982.
(59) Hospital-Benito, D.; Lemus, J.; Moya, C.; Santiago, R.; Palomar, J. Process Analysis Overview of Ionic Liquids on CO_2 Chemical Capture. *Chem. Eng. J.* **2020**, *390*, 124509.
(60) Moreno, D.; Ferro, V. R.; de Riva, J.; Santiago, R.; Moya, C.; Larriba, M.; Palomar, J. Absorption Refrigeration Cycles Based on Ionic Liquids: Refrigerant/Absorbent Selection by Thermodynamic and Process Analysis. *Appl. Energy* **2018**, *213*, 179−194.
(61) Chaudhari, S. K.; Salavera, D.; Esteve, X.; Coronas, A. Vapour−Liquid Equilibria of the System 1,1,1,2-Tetrafluoroethane + Monoethylene-Glycol Dimethylether from 283.15 to 353.15 K: New Modified UNIFAC Parameters. *Fluid Phase Equilib.* **2008**, *271*, 28−33.
(62) Sousa, J. M. M. V.; Almeida, J. P. B.; Ferreira, A. G. M.; Fachada, H. C.; Fonseca, I. M. A. Solubility of HFCs in Lower Alcohols. *Fluid Phase Equilib.* **2011**, *303*, 115−119.
(63) Tseregounis, S. I.; Riley, M. J. Solubility of HFC-134a Refrigerant in Glycol-type Compounds: Effects of Glycol Structure. *AIChE J.* **1994**, *40*, 726−737.
(64) Sousa, J. M. M. V.; Queimada, A. J.; Macedo, E. A.; Fonseca, I. M. A. Solubility of Hydrofluorocarbons in Aromatic Solvents and Alcohols: Experimental Data and Modeling with CPA EoS. *Fluid Phase Equilib.* **2013**, *337*, 60−66.
(65) Liu, Y.; Jiang, L.; Wang, H.; Wang, H.; Jiao, W.; Chen, G.; Zhang, P.; Hui, D.; Jian, X. A Brief Review for Fluorinated Carbon: Synthesis, Properties and Applications. *Nanotechnol. Rev.* **2019**, *8*, 573−586.
(66) Ferreira, M. L.; Pastoriza-Gallego, M. J.; Araújo, J. M. M.; Canongia Lopes, J. N.; Rebelo, L. P. N.; M. Piñeiro, M. M.; Shimizu, K.; Pereiro, A. B. Influence of Nanosegregation on the Phase Behavior of Fluorinated Ionic Liquids. *J. Phys. Chem. C* **2017**, *121*, 5415−5427.
(67) Carvalho, P. J.; Kurnia, K. A.; Coutinho, J. A. P. Dispelling Some Myths about the CO2 Solubility in Ionic Liquids. *Phys. Chem. Chem. Phys.* **2016**, *18*, 14757−14771.

https://doi.org/10.1021/acs.est.2c00051
Environ. Sci. Technol. 2022, 56, 5898−5909